Sager, W.W., Kanazawa, T., and Escutia, C. (Eds.)
Proceedings of the Ocean Drilling Program, Scientific Results Volume 191

1. Leg 191 Synthesis: Summary of Scientific Results[1]

William W. Sager[2] and Carlota Escutia[3]

ABSTRACT

Ocean Drilling Program (ODP) Leg 191 was devoted mainly to two engineering goals, installing a borehole seismometer inside a cased hole and tests of the hard rock reentry system. Those results were achieved, and the borehole seismometer has already yielded useful seismological data showing that the observatory has a low noise profile rivaling quiet land stations. In preparation for emplacing the observatory casing, several holes were drilled at the observatory site (Site 1179), penetrating a 375-m-long sedimentary section and 100 m of igneous crust. Cores from these two sections have been used for a suite of ancillary studies that improve our knowledge of the tectonics and properties of the crust as well as changes in North Pacific climate. Studies of the sedimentary section include investigations of biostratigraphy, anomalous high-carbonate content layers, discrete ash layer chronology and stratigraphy, sediment geochemistry, porosity and permeability, gamma ray logs, and anisotropy of magnetic properties. Among other things, these studies imply that the sedimentary column has a significant terrigenous component, despite the distance from land, and that there were periods when this input fertilized surface waters and stimulated surface productivity. Studies of the igneous basement include investigations of isotopic ratios and paleomagnetism. Nd and Sr isotope ratios suggest that the crust is distinct from normal mid-ocean-ridge basalts, perhaps because of the influence of a nearby plume that may have formed Shatsky Rise. Paleomagnetic data indicate that Site 1179 formed within a few degrees of the equator and has drifted ~39° northward. In sum, Leg 191 postcruise science investigations add to the legacy of Pacific geologic data with contributions that will help understand Pacific sediments, igneous crust, and environment.

[1]Sager, W.W., and Escutia, C., 2005. Leg 191 synthesis: summary of scientific results. *In* Sager, W.W., Kanazawa, T., and Escutia, C. (Eds.), *Proc. ODP, Sci. Results,* 191, 1–19 [Online]. Available from World Wide Web: <http://www-odp.tamu.edu/publications/191_SR/VOLUME/SYNTH/SYNTH.PDF>. [Cited YYYY-MM-DD]
[2]Department of Oceanography, Texas A&M University, College Station TX 77843-3146, USA.
wsager@ocean.tamu.edu
[3]Instituto Andalúz de Ciencias de la Tierra, CSIC-Universidad de Granada, 18002 Granada, Spain.

Initial receipt: 2 December 2003
Acceptance: 19 November 2004
Web publication: 20 May 2005
Ms 191SR-001

INTRODUCTION

Ocean Drilling Program (ODP) Leg 191 was a cruise devoted primarily to engineering, specifically the emplacement of a borehole seismometer beneath the abyssal plain of the northwest Pacific Ocean and testing of the hard rock reentry system (HRRS; also known as the "hammer drill"). Only one site was drilled for science (Site 1179), and therefore logging, coring, and studies of core samples were secondary goals of the expedition. The ship carried only a small contingent of scientists whose research involved the study of core or logging data, and as a result the number of postcruise science contributions cannot be easily melded into a scientifically focused theme. This chapter describes postcruise science from Site 1179 as a guide for the reader of this volume. Results from HRRS testing are not described here because the engineering tests resulted in progress reports but no samples were recovered, and, hence, no scientific papers were produced from this aspect of drilling.

Initial Results Recap

Site 1179 was drilled on abyssal seafloor, at a depth of 5564 meters below sea level (mbsl), located on magnetic Anomaly M8, ~240 km northwest of Shatsky Rise in the northwest Pacific Ocean (Fig. F1). A 375-m-thick sedimentary section was cored before penetrating 100 m into the upper oceanic crust. Although a total of five holes (1179A through 1179E) were drilled at the site, coring was done in only two, Holes 1179B and 1179C (Shipboard Scientific Party, 2001a).

The Site 1179 sedimentary section consists of four distinct units (Figs. F2, F3). The uppermost unit is a thick (221.5 m) layer of late Miocene to late Pleistocene age consisting of clay- and radiolarian-bearing diatom ooze. Considering the distance from land and generally low mid-ocean sedimentation rates, this unit is anomalously thick. It appears to be thickest in the waters east of Japan and probably results from high productivity related to the Kuroshio Current and its convergence with the Oyashio Current (Shipboard Scientific Party, 2001a). The diatom ooze sits atop a 24.5-m-thick layer of clay-rich, diatom-bearing radiolarian ooze of late Miocene age, which in turn rests on a 37.5-m-thick layer of barren brown pelagic clay of uncertain age. Within lithostratigraphic Units I and II, 13 discrete vitric ash layers were identified (Shipboard Scientific Party 2001a). The lowermost unit consists of chert layers within a unknown host sediment. The host sediment is unknown because only chert fragments were recovered within the 93.7-m unit above igneous basement. The age of the sediment is known to include the Early Cretaceous because of a few specimens of radiolarian tests that were recovered from chert fragments.

Physical properties of the Miocene and younger sediments are unusual because of the high content of diatom frustules. These low-density silica particles have high porosity and, as a result, the Unit I sediments have unusually high porosity and low density for sediments buried by tens or hundreds of meters of sediment. Nevertheless, these sediments produced a useful magnetic stratigraphy as well as a biostratigraphy based mainly on radiolarian assemblages with a few datums from dinoflagellates and one from an anomalous layer of nannofossils (Shipboard Scientific Party, 2001b). Age data from the different fossil types are in good agreement and indicate slow sedimentation in the

F1. Site 1179 location, p. 11.

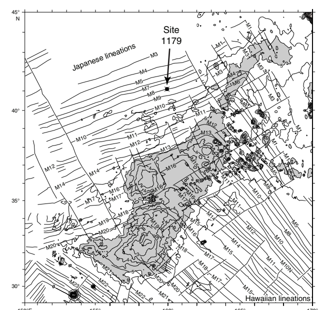

F2. Lithostratigraphic summary, Site 1179, p. 12.

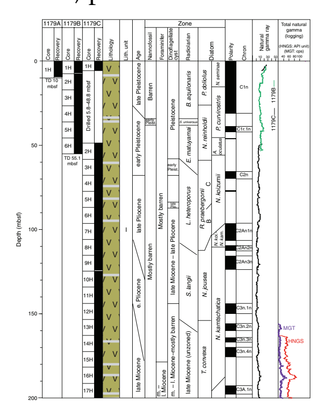

F3. Stratigraphy at Site 1179 and other northwest Pacific boreholes, p. 15.

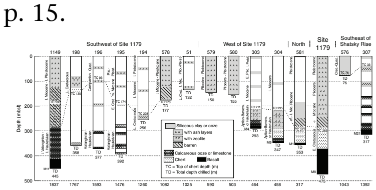

Miocene (~2 m/m.y.), which gave way to rapid sedimentation in the last 5 m.y. (40–43 m/m.y.).

Basement coring was reasonably successful, with 43.5% recovery over the 100-m interval cored. Recovered igneous rock mostly consists of aphyric basalts in massive flows, pillows, and breccia. Based on lithologic and textural differences, sediment interbeds, and flow and cooling unit boundaries, the basement section was divided into 48 units. Furthermore, it was also possible to divide the igneous section into three different groups, based on the abundance of the mineral olivine. The uppermost 8 units consist of olivine-poor basalts, whereas the middle 16 units are characterized by olivine-free basalts and the lower 24 units are olivine-rich basalt (Shipboard Scientific Party, 2001b). Alteration of the igneous rocks appears low in hand specimens and thin sections, which indicated zeolite facies metamorphism and temperatures below 30°C.

Logging data from Leg 191 were few because only one site was drilled and there were hole stability problems in Hole 1179D, the single hole logged. Although the first tool string was initially lowered to 300 meters below seafloor (mbsf), the run was reversed for calibration tests and a bridge developed at 260 mbsf, thwarting attempts to log deeper in the hole (see Fig. F2).

POSTCRUISE SCIENTIFIC RESULTS

Sedimentary Section Studies

Biostratigraphy and Paleoceanography

Two studies investigated the fossil record in Site 1179 sediments. Winter et al. (this volume) developed a biostratigraphy from diatoms (Fig. F4). This study complements the shipboard biostratigraphy, which was based primarily on radiolarians and dinoflagellates. The authors report that preservation of diatom frustules is good, with abundances ranging from rare to abundant and no barren samples encountered. Because the sediments contain both tropical and temperate diatom species, it was possible to correlate the fossil assemblages with those of equatorial and North Pacific biostratigraphies. The succession of diatoms appears nearly complete, with only one zonal boundary missing. Furthermore, it agrees well with the previously defined shipboard biostratigraphy. Diatom abundance was found to be lower in the Miocene and greater in the Pliocene and Pleistocene, consistent with shipboard observations of an increase in siliceous sedimentation with time as Site 1179 came under the influence of the Kuroshio Current.

F4. Diatom biostratigraphy, p. 16.

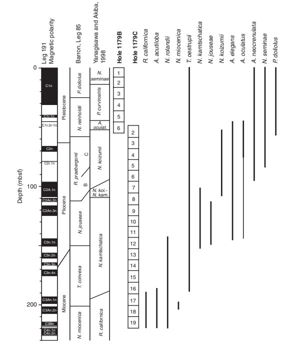

McCarthy and coworkers (McCarthy et al., 2004a, 2004b) examine the implications of several calcareous layers that occur in the otherwise siliceous sediment section of Site 1179 at depths of ~37, 61, and 92 mbsf, corresponding to ages of 0.7–0.9, 1.6, and 2.4–2.5 Ma, respectively. These layers were deposited >1 km below the carbonate compensation depth (CCD) and contain well-preserved foraminifer tests, including some dissolution-prone species. These layers also contain synchronous peaks of pollen that indicate aridification and cooling, leading the authors to conclude that the layers were deposited during glacial periods. These layers correspond to similar high carbonate content layers found in other North Pacific sediment cores recovered during ODP Leg 145 and with sections of Chinese loess in mainland Asia.

The authors explain the layers by fertilization of surface waters by dust from Asia (containing growth-limiting nutrients) during glacial periods with strong winds. The result was higher productivity in surface waters and concomitant high sedimentation at the seafloor, allowing the carbonate sediments to be deposited and buried before dissolution could remove them. McCarthy and coworkers (2004a) speculate that these brief periods of high sedimentation were widespread and that the sequestration of carbon dioxide in carbonate sediments may have augmented global cooling during these times by reduction of the greenhouse effect. The authors also note that the palynological record is key to recognizing the provenance and paleoclimate implications of terrigenous particles blowing to the ocean from Asia.

Sediment Properties

Using X-ray absorption techniques, Fukukawa et al. (this volume) measured major element and rare earth element abundances for sediment samples from the upper 35 m of Site 1179. In particular, they examined the oxidation state of Mn and Ce and the effect of element abundances on several geochemical ratios used as provenance indicators. Mn is reduced to Mn(II) below 0.6 mbsf, with low abundance in sediments and high abundance in pore waters. The authors concluded that the Mn/TiO_2 ratio, often used to deduce depositional environment, must be affected by diagenesis. In contrast, the ratio La/Ce changes little with depth, suggesting it is not significantly affected by diagenesis. On a plot of La/Ce vs. $Al_2O_3/(Al_2O_3+Fe_2O_3)$, used to infer sediment source region, Site 1179 samples plot between continental and pelagic zones, leading the authors to conclude that there is significant terrigenous input to the sediments, despite the distance of Site 1179 from land.

Arguing that knowledge of sediment permeability and porosity is critical to understanding fluid flow, Kwon et al. (this volume) made transient pulse method measurements of permeability and porosity for six sediment samples from Site 1179. Both quantities are high for Units I and II (porosities >80% and permeabilities of 342–1779 µD), consistent with physical property measurements made on these diatomaceous sediments during Leg 191. The single sample measured from Unit III, the pelagic brown clay, had much lower porosity (~66%) and permeability (1.9 µD).

The data report by Horner-Johnson and Sager (this volume) presents anisotropy data for anhysteretic remanent magnetization and magnetic susceptibility. According to previous studies, anisotropy is low in sediments that have low compaction but increases in sediments that have compacted as magnetic grains rotate to the same plane with vertical shortening. The authors find that in Units I and II, the high porosity, low-density diatomaceous section, anisotropies are low and near isotropic. In contrast, sediments in the pelagic brown clay, Unit III, show oblate spheroid (pancake shaped) distributions of anisotropy, indicating significant effects of compaction and implying that magnetic grains have been rotated toward the horizontal plane. This finding suggests that Unit III sediments are probably ill-suited for determining paleomagnetic inclination, owing to possible rotation of the magnetic vector.

Ash Chronology and Stratigraphy

Escutia et al. (unpubl. data) recognized 14 volcanic events within the upper 200 m of the sedimentary section (Unit I) at Site 1179 (Figs. F2, F5). They conducted radiometric dating on some of the ash layers using $^{39}Ar/^{40}Ar$ radiometric dating techniques for ash shards. Other ash-layer dates were derived by comparing the $^{40}Ar/^{39}Ar$ chronology framework to magnetostratigraphy for Site 1179 (and also northwest Pacific Site 1149) (see Escutia et al., unpubl. data). The refined chronology will be invaluable for future geochemical and volcanologic studies to determine the evolution of arc volcanism in the northern circum-Pacific. It allowed the authors to study the stratigraphic evolution of the northwestern Pacific since Messinian time (Escutia et al., in press).

Results from the ash study are relevant to "subduction factory" studies because of their bearing on the composition and total cumulative thickness of ash being subducted in the Kurile Trench. Tephras from Site 1179 are chemically bimodal (i.e., basaltic and rhyolitic), with rhyolitic volcanic events dominating during Messinian and early Pliocene times (i.e., 4.3–5.3 Ma) and through most of the Quaternary. Cumulative thickness of ash at Site 1179 is ~1 m, ~0.5% of the total sediment deposited during the last 7 m.y. Taking into account the mass fraction of dispersed ash in the background sediment, as indicated by nonquantitative shipboard smear slide estimates, the total cumulative thickness of ash in the sediment column that will be subducted in the Kurile Trench could vary between 3 and 13 m, or 1.5% and 6.5%.

Relevant to paleoceanographic and paleoclimatic studies are the inferred sedimentation rates at Site 1179, which exhibit a nearly linear increase from the Messinian (24 m/m.y.) to the late Pleistocene (31.6 m/m.y.). Such high sedimentation rates, at an oceanic site distant from land sources, are attributed to high productivity in nutrient-rich waters that characterizes the area of convergence between the Kuroshio Front and the Oyashio Current, where Site 1179 is located. An increase in sedimentation rates (from 27.4 to 38.6 m/m.y.) during the late Pliocene at ~2.5–3.0 Ma coincides with maximum frequency of volcanic events at this site (2.1 and 2.5 Ma) and with one of the maximum peaks in cumulative ash thickness. Interestingly, this time (3.0–2.5 Ma) coincides with the cooling trend associated with the initiation of Northern Hemisphere glaciation. The coincidence of high sedimentation rates and high input of volcanic ash observed at ~2.5 Ma at Site 1179 is interpreted by Escutia et al. (in press) to be the result of climatic cooling related to increased volcanic activity. Cooling may have resulted in stronger winds, bringing more ash and dust from an increasingly arid Asia. In addition, these conditions proved more favorable for the growth of diatoms in the northwest Pacific, leading to greater deposition of siliceous tests.

F5. Ash layer chronology, p. 17.

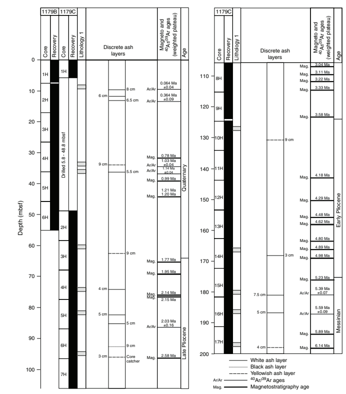

Igneous Oceanic Crust Studies

Isotope Geochemistry

Sano and Hayasaka (this volume) measured Sr and Nd isotope compositions of 19 basalt samples from Site 1179 basement. Initial ratios range $^{84}Sr/^{86}Sr$ = 0.7029–0.7040 and $^{143}Nd/^{144}Nd$ = 0.5131–0.5132 (ε_{Nd}(t) = 9.3–10.8), but age corrections change the values for Sr to 0.7026–0.7033 and ε_{Nd}(t) to 9.2–10.6. Plotting these data relative to one another (Fig. F6) shows that the Sr ratio is higher than the normal Sr ratio of

F6. εNd(t) vs. $^{87}Sr/^{86}Sr$, p. 18.

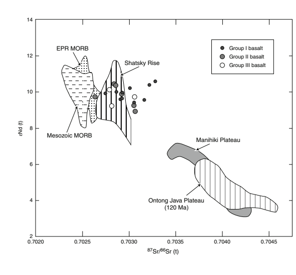

mid-ocean-ridge basalt (MORB), implying that crust at Site 1179 may have been affected by plume volcanism from nearby Shatsky Rise, which was active at the same time the Site 1179 crust formed. This result is similar to previously published findings from crustal basalt cored at nearby Deep Sea Drilling Project (DSDP) Site 304 (Janney and Castillo, 1997).

Radiometric Dating

Initial description of the igneous section indicated that alteration in the basement rocks is low, raising hopes that a high-precision radiometric date would be determined (Shipboard Scientific Party, 2001b). Because Site 1179 is near the middle of a well-defined magnetic isochron (M8), such a date would be important as a tie-point for the geomagnetic polarity reversal timescale. Unfortunately, this effort did not work as hoped.

The radiometric dating analysis was done by Anthony Koppers using techniques for ^{39}Ar/^{40}Ar dating of altered sample groundmass that have given accurate results with other seawater-altered basalts (Koppers et al., 2000). He analyzed three samples, and two gave age plateaus, but with values of 103–105 Ma, which do not appear reasonable for rocks of M8 age (~129 Ma by the Gradstein et al., 1995, timescale). He gives several reasons why the calculated ages appear inaccurate (A. Koppers, pers. comm., 2004). K/Ca ratios of the rocks are extremely low and indicate that there is virtually no primary K residing in the rock grains. The existing K was probably introduced by seawater alteration. Age plateaus are short and show evidence for extreme ^{39}Ar recoil, which is common for samples with pervasive fine-grained alteration. Furthermore, total fusion ages are extremely discordant (~140–160 Ma), implying that the Ar system has not been closed, violating a fundamental condition needed for reliable age determination

Paleomagnetism

Noting that paleomagnetic results from Site 1179 could be important because few Pacific boreholes have penetrated as deep as 100 m into oceanic basement, Sager and Horner-Johnson (this volume) studied 122 basalt samples from 41 of 48 igneous units. Although the number of units appears large, statistical comparison implied that the data comprise only 13 independent magnetic units (i.e., units between which significant time has passed for secular variation of the geomagnetic field to occur) (Fig. F7). This implies that many flows are serially correlated and probably erupted within a short time of one another. Indeed, all of the units in the lower 33 m of the section were statistically indistinguishable, indicating that units in flow group 3 (olivine-rich basalts) were emplaced rapidly. From the 13 independent measurements, a mean paleolatitude of 1.9°N ± 6.8° was determined, assuming the negative inclinations of most samples represent a reversed magnetic polarity formed north of the equator. This paleolatitude implies that the crust at Site 1179 formed near the equator and has drifted ~39° northward since then. The authors caution that uncertainty in the paleolatitude remains because the 13 independent units may not have completely averaged secular variation; nonetheless, the paleolatitude results are important because they can be used in compilations of Pacific paleomagnetic data (e.g., Sager, in press).

F7. Measured and flow mean colatitudes, p. 19.

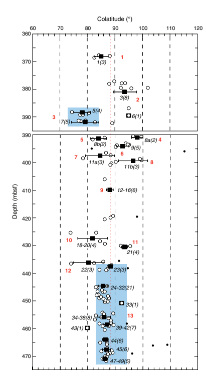

In a separate data report, Sager (this volume) reports measurements made on basalt samples from eight other sites drilled during prior DSDP and ODP cruises. Most of these cores were previously overlooked because they sampled only a few igneous units and therefore were unlikely to produce unequivocal paleolatitude results. However, as noted above, such data are nonetheless valuable when averaged with other coeval data (Sager, in press). Sager (this volume) reports results from three holes from DSDP Leg 17, one hole common to DSDP Legs 86 and 88, and one hole each from DSDP Leg 92 and ODP Legs 129, 130, and 143.

Logging Studies

Goldberg et al. (this volume) analyzed data from the Multi-sensor Spectral Gamma Ray Tool (MGT), a new, high-resolution gamma ray logging device deployed for the first time during Leg 191. These data were compared with lower-resolution data from the standard gamma ray logging tool (Hostile Environment Gamma Ray Sonde; HNGS). Logs from the two different sensors agreed in overall shape, but the vertical resolution of the MGT was several times better than the HNGS. Differences between concentrations of radioactive elements K, U, and Th estimated from the two sensors caused some concern and were blamed on differences in the borehole between logging runs, low radioactive element concentrations in the sediments, and differences in processing algorithms. The authors conclude that the new tool will be useful for high-resolution studies, especially the correlation of thin clay beds between core and logging data.

Seismometer Studies

The information presented in this section is paraphrased from a report detailing progress on two western Pacific borehole seismic observatories set up by ODP, including the WP-2 observatory at Site 1179 (Shinohara et al., in press). After installation during July and August of 2000, the WP-2 observatory was visited by a remotely operated vehicle (ROV), which activated the equipment on 29 October 2000. Subsequent ROV visits in January 2001 and June 2002 retrieved data recordings totaling 417 days. Because the initial data set indicated that the vertical channel on the seismometer was somewhat noisy and had an unexpected spectral response, it was switched off and a backup vertical unit was activated. It is thought that the original vertical sensor may have been damaged during installation, but this supposition cannot be tested because the sensors are cemented in the Site 1179 borehole.

Analysis of WP-2 data indicates that the borehole noise spectrum is similar to other submarine borehole observatories and is comparable with quiet stations on land. In particular, the long-period noise shows little time variation, which allows more reliable comparisons of different event records. Noise from ocean waves appears attenuated over seafloor installations, a result of installing the sensors within a basement borehole. Noise with a period of several seconds is observed by the observatory and is thought to be related to wind stress over the ocean.

Many seismic events have been recorded by the WP-2 observatory, including both local and teleseismic events. Comparison with published earthquake records indicates that the WP-2 observatory can distinguish distant events with magnitudes (M) > 5. For earthquakes in the local region, the observatory shows even smaller events, with magnitudes as low as M = ~4.

CONCLUSIONS

Postcruise science from ODP Leg 191 consists mainly of data recovery and initial study of seismic data from the observatory and studies of the sedimentary and igneous sections cored in Site 1179. A study of diatoms defined a nearly continuous biostratigraphy that is similar to shipboard biostratigraphies based on radiolarians and dinoflagellates. Studies of several anomalous carbonate-rich layers in the Pliocene–Pleistocene section suggest that terrigenous dust from Asia caused plankton blooms by supplying nutrients that caused high productivity and sedimentation during several glacial periods. The rapid sequestration of carbonate in seafloor sediments at this time may have augmented global cooling. The conclusion that Site 1179 sediments contain a terrigenous component is bolstered by a sedimentary geochemistry study that shows element ratios that are between true pelagic and continental values. This same study also shows that Mn is depleted downsection by diagenesis and that Mn abundance ratios, sometimes used to infer sediment provenance, may not be reliable. Other sedimentary studies show the effects of the downsection decrease in diatom content and increase in compaction on permeability, porosity, and magnetic grain orientation. $^{40}Ar/^{39}Ar$ dating of vitric shards in discrete ash layers provides a new combined $^{40}Ar/^{39}Ar$ and magnetostratigraphic chronology at Site 1179 for the past 6.2 m.y. The 14 ash layers correspond to 14 major volcanic episodes on land since late Miocene (Messinian) time. The increase in sedimentation rates at ~2.5–3.0 Ma, coinciding with maximum frequency of volcanic events and with peaks in cumulative ash thickness, is interpreted to result from increased dust and ash transport by stronger winds to Site 1179, likely associated with cool climates. Tephras within the sediment column to be subducted in the Kurile Trench are chemically bimodal (i.e., rhyolitic and basaltic), with a total thicknesses of ash in discrete ash layers estimated to be ~1 m (~0.5%) of the total sediment at Site 1179. The total thickness of volcanigenic material is estimated to be 3–13 m (1.5%–6.5%) if the mass fraction of dispersed ash in the background sediment is also considered. Natural gamma ray logs in the sedimentary section show the utility of a new high-resolution logging tool. Igneous section geochemistry and isotope ratios imply that Site 1179 basalts have higher Sr isotope ratios than normal MORB, perhaps owing to the influence of a plume that was building Shatsky Rise near the ridge when the crust at Site 1179 was formed. Paleomagnetic data from the igneous section indicate that the lower basalts were emplaced rapidly and that the crust formed near the equator.

Because the main objective of Leg 191 was to emplace a seismometer and to conduct engineering tests, the results from research in samples and data from this site are not geared to solve a particular scientific problem or to test a hypothesis but are nonetheless relevant to the understanding of the paleoceanographic evolution, history of volcanic arc volcanism, subduction factory studies, and formation and evolution of the oceanic crust, among other topics. In addition, the sedimentary section at Site 1179 is very similar to the one recovered from Site 1149, located just east of the Izu-Bonin Trench. Both Sites 1149 and 1179 are locations where the two most complete sedimentary sections have been recovered from the northwestern Pacific. Future comparative studies between these two sites thus have the potential to augment the results presented in this synthesis.

ACKNOWLEDGMENTS

This research used samples and/or data provided by the Ocean Drilling Program (ODP). ODP is sponsored by the U.S. National Science Foundation (NSF) and participating countries under management of Joint Oceanographic Institutions (JOI), Inc. We thank Ralph Moberly for a conscientious review of this manuscript.

REFERENCES

Barron, J.A., 1985. Late Eocene to Holocene diatom biostratigraphy of the equatorial Pacific Ocean, Deep Sea Drilling Project Leg 85. *In* Mayer, L., Theyer, F., Thomas, E., et al., *Init. Repts. DSDP,* 85: Washington (U.S. Govt. Printing Office), 413–456.

Escutia, C., Gutiérrez-Pastor, J., and Canon, M., in press. Tephra stratigraphy in northwestern Pacific since the Messinian: ODP Sites 1149 and 1779. *Mar. Geol.*

Gradstein, F.M., Agterberg, F.P., Ogg, J.G., Hardenbol, J., van Veen, P., Thierry, J., and Huang, Z., 1994. A Mesozoic time scale. *J. Geophys. Res.,* 99:24051–24074.

Janney, P.E., and Castillo, P., 1997. Geochemistry of Mesozoic Pacific mid-ocean ridge basalt: constraints on melt generation and the evolution of the Pacific upper mantle. *J. Geophys. Res.,* 102:5207–5229.

Kanazawa, T., Sager, W.W., Escutia, C., et al., 2001. *Proc. ODP, Init. Repts.,* 191 [CD-ROM]. Available from: Ocean Drilling Program, Texas A&M University, College Station TX 77845-9547, USA.

Koppers, A.A.P., Staudigel, H., and Wijbrans, J.R., 2000. Dating crystalline groundmass separates of altered Cretaceous seamount basalts by the $^{40}Ar/^{39}Ar$ incremental heating technique. *Chem. Geol.,* 166:139–158.

McCarthy, F.M.G., Findlay, D.J., and Little, M.L., 2004a. The micropaleontological character of anomalous calcareous sediments below the CCD in the northwestern North Pacific Ocean. *Palaeogeogr., Palaeoclimatol., Palaeoecol.,* 215:1–15.

McCarthy, F.M.G., Gostlin, K.E., Mudie, P.J., and Ohlenschlager Pedersen, R., 2004b. The palynological record of terrigenous flux to the deep sea: late Pliocene–Recent examples from 41°N latitude in the abyssal Atlantic and Pacific Oceans. *Rev. Paleobot. Palynol.,* 128:81–95.

Nakanishi, M., Sager, W.W., and Klaus, A., 1999. Magnetic lineations within Shatsky Rise, northwest Pacific Ocean: implications for hot spot–triple junction interaction and oceanic plateau formation. *J. Geophys. Res.,* 104:7539–7556.

Sager, W.W., in press. DSDP and ODP basalt core paleomagnetic poles for the Cretaceous Pacific plate: implications for apparent polar wander and plate tectonics. *Phys. Earth Planet. Int.*

Sager, W.W., Kim, J., Klaus, A., Nakanishi, M., and Khankishieva, L.M., 1999. Bathymetry of Shatsky Rise, northwest Pacific Ocean: implications for ocean plateau development at a triple junction. *J. Geophys. Res., [Solid Earth Planets],* 104:7557–7576.

Shipboard Scientific Party, 2001a. Leg 191 summary. *In* Kanazawa, T., Sager, W.W., Escutia, C., et al., et al., *Proc. ODP, Init. Repts.,* 191: College Station TX (Ocean Drilling Program), 1–49.

Shipboard Scientific Party, 2001b. Site 1179. *In* Kanazawa, T., Sager, W.W., Escutia, C., et al., *Proc. ODP, Init. Repts.,* 191, 1–159 [CD-ROM]. Available from: Ocean Drilling Program, Texas A&M University, College Station TX 77845-9547, USA.

Shinohara, M., Araki, E., Kanazawa, T., Suyehiro, K., Mochizuki, M., Yamada, T., Nakahigashi, K., Kaiho, Y., and Fukao, Y., in press. Deep-sea borehole seismological observatories in the western Pacific: temporal variation of seismic noise level and event detection. *Ann. Geoph*ys.

Yanagisawa, Y., and Akiba, F., 1998. Refined Neogene diatom biostratigraphy for the northwest Pacific around Japan, with an introduction of code numbers for selected diatom biohorizons. *J. Geol. Soc. Jpn.,* 104:395–414.

Figure F1. Site 1179 location. Gray areas show bathymetry above 5000 m depth (Sager et al., 1999), highlighting the Shatsky Rise ocean plateau. Lines show magnetic lineations and fracture-zone offsets (Nakanishi et al., 1999). Solid circle shows the location of Site 1179 (modified from Kanazawa, Sager, Escutia, et al., 2001).

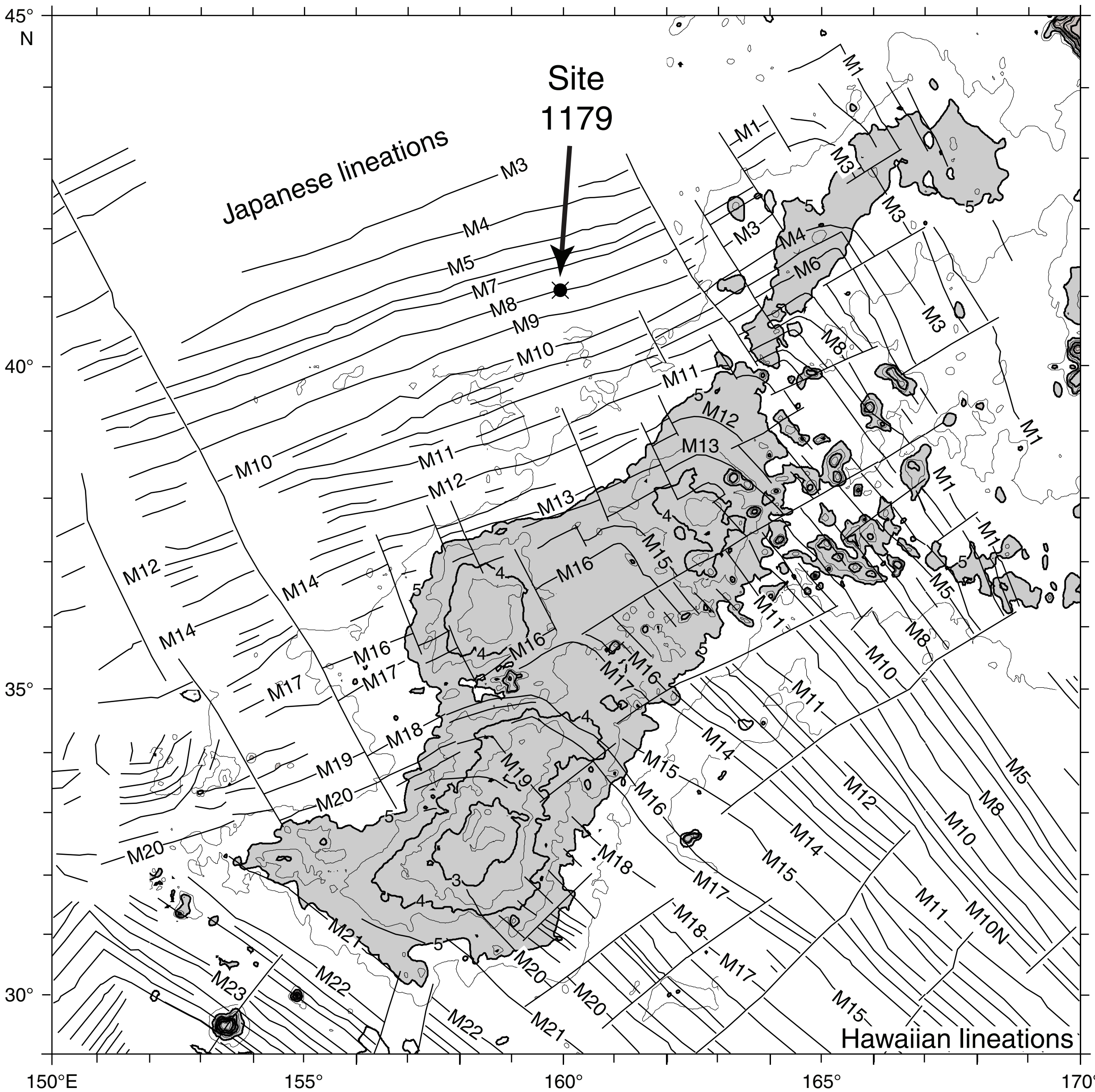

Figure F2. Lithostratigraphic summary for Site 1179. Core recovery is shown in left columns, with solid blocks indicating the amount of recovered core. Lithology and lithostratigraphic unit columns show generalized stratigraphy. Lightly shaded bands in Unit I lithology column represent ash layers. Magnetic polarity is shown by black (normal polarity) and white (reversed polarity) bands. Chron age designations are given next to the polarity column. Curves in far right columns are from downhole logs (modified from Kanazawa, Sager, Escutia, et al., 2001). HNGS = Hostile Environment Gamma Ray Sonde, MGT = Multi-Sensor Spectral Gamma Ray Tool, TD = total depth. (Continued on next two pages.)

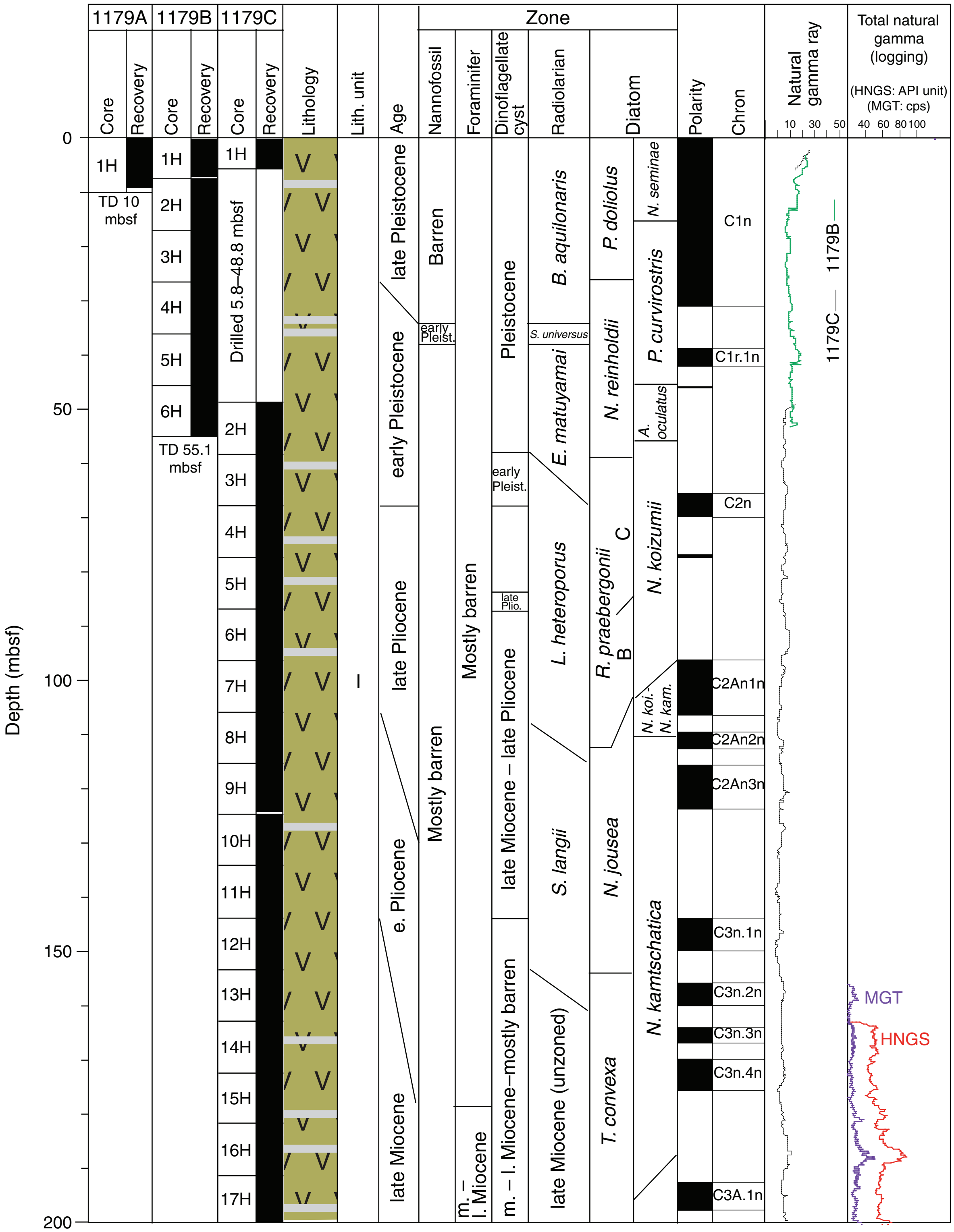

Figure F2 (continued).

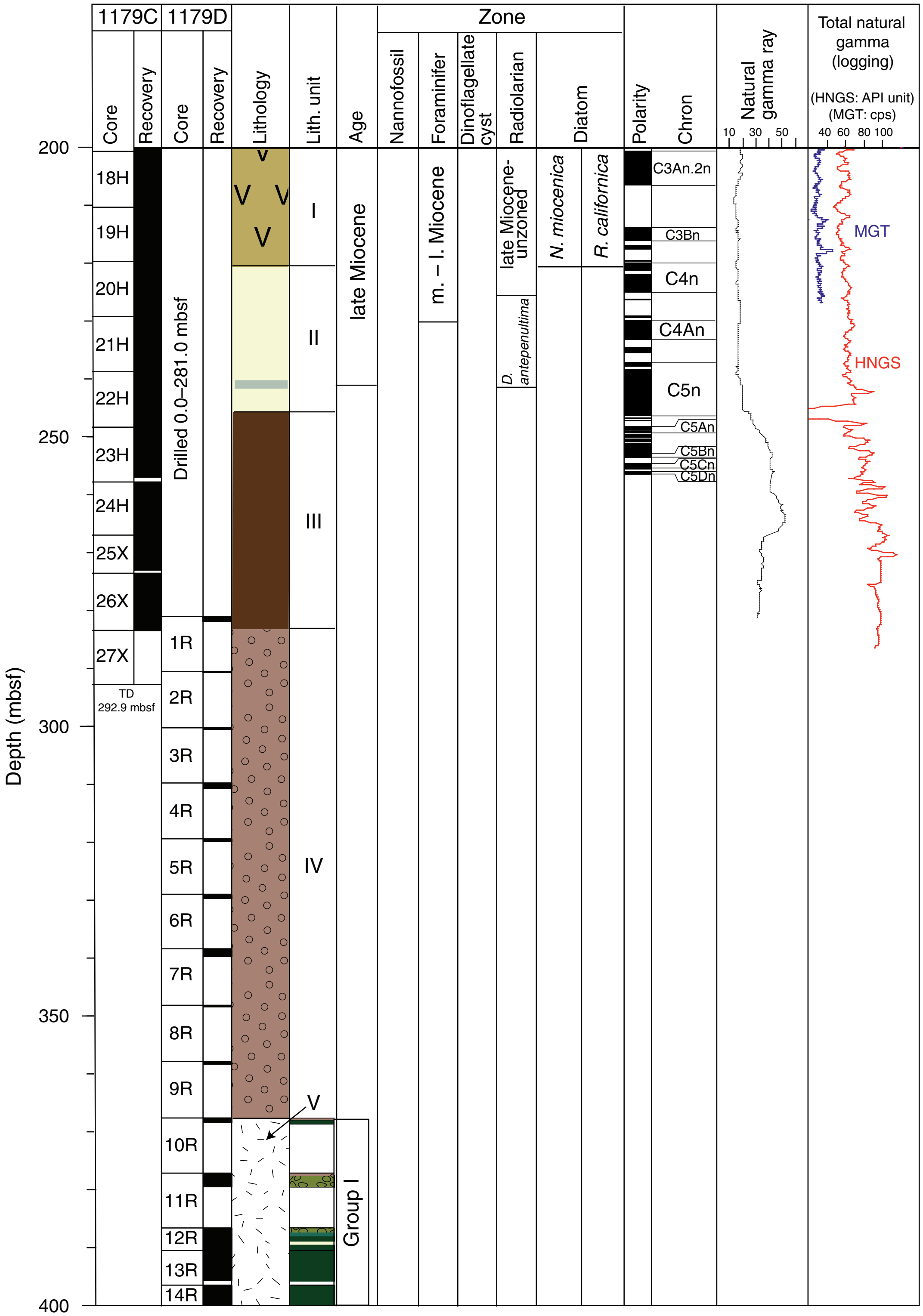

Figure F2 (continued).

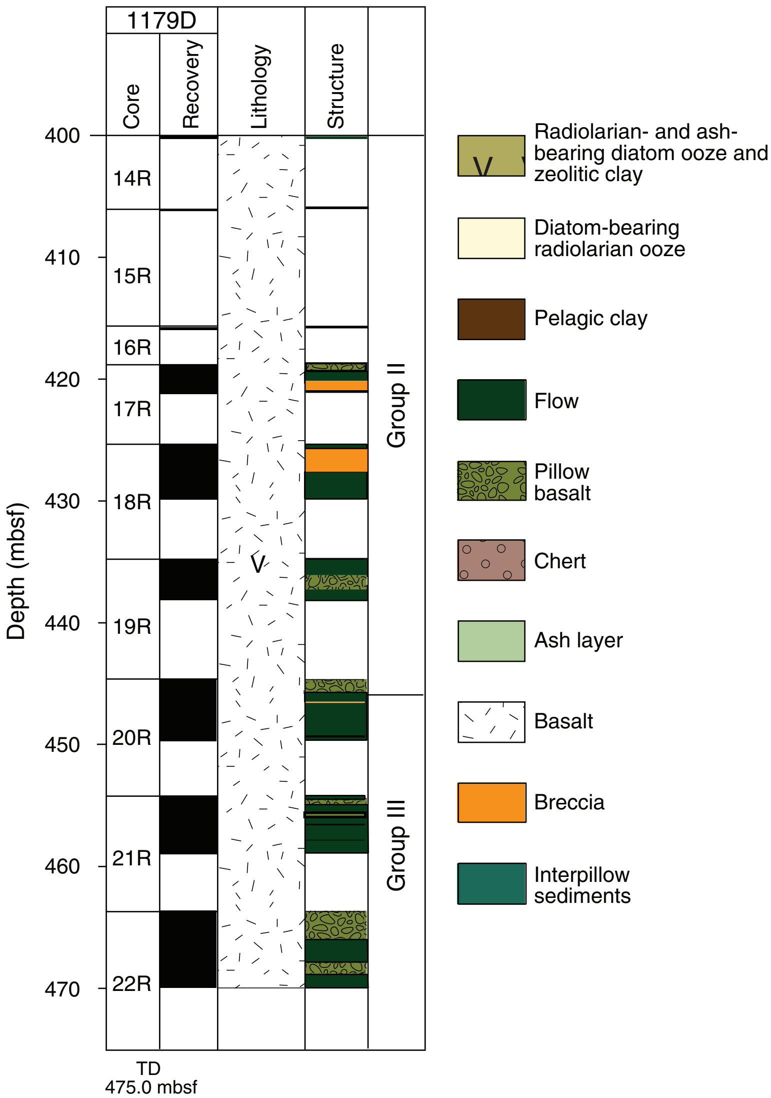

Figure F3. Graphic comparison of stratigraphic columns at Site 1179 and other DSDP and ODP boreholes in the northwest Pacific. Numbers at top give site designations. Biostratigraphic ages are given along the left side of each column. Inclined dotted lines show the contact between Cretaceous and Cenozoic sediments. The distance from Site 1179 is shown at the bottom (from Kanazawa, Sager, Escutia, et al., 2001).

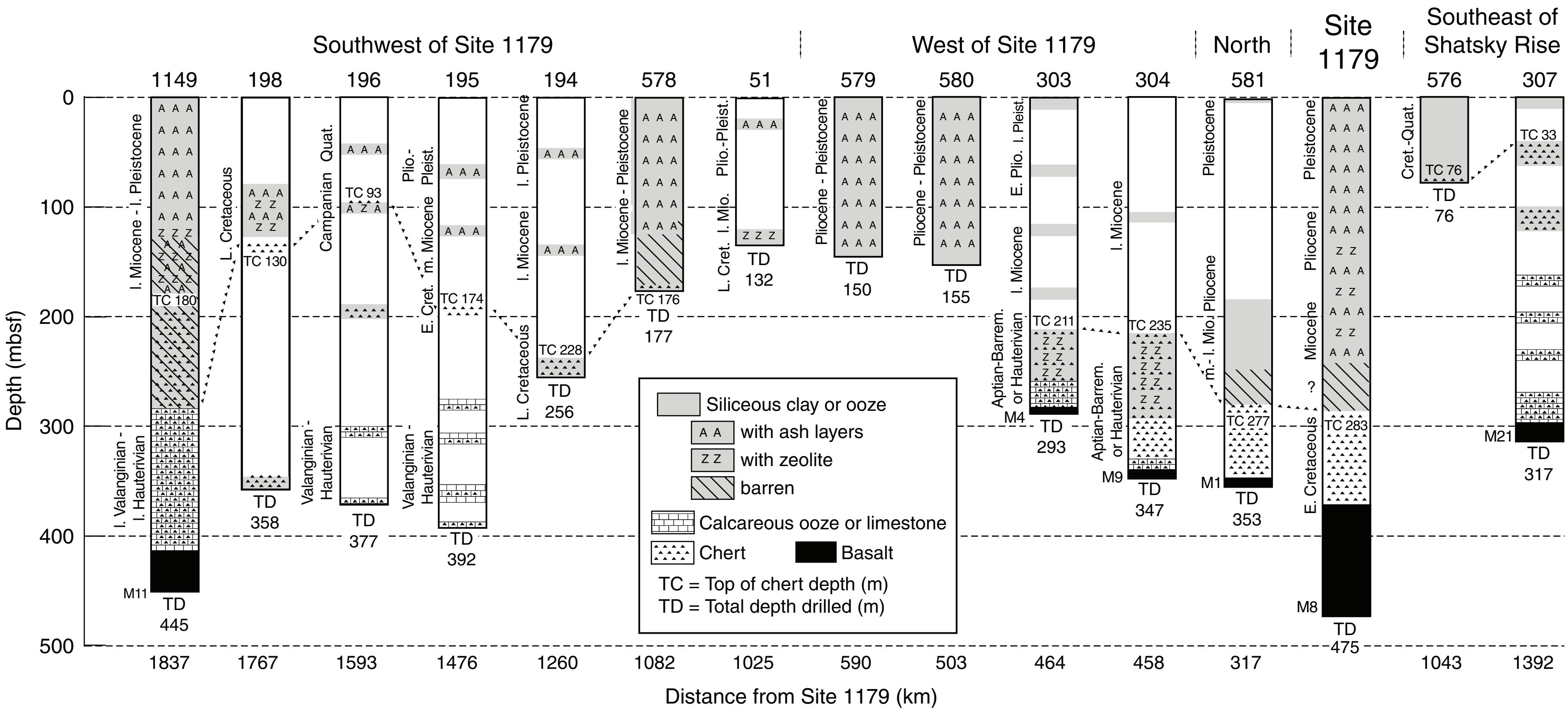

Figure F4. Diatom biostratigraphy for Holes 1179B and 1179C. Columns at left are biozones from prior publications. Middle columns represent cores from Holes 1179B and 1179C. Vertical lines at right represent occurrences of marker fossils (from Winter et al., this volume).

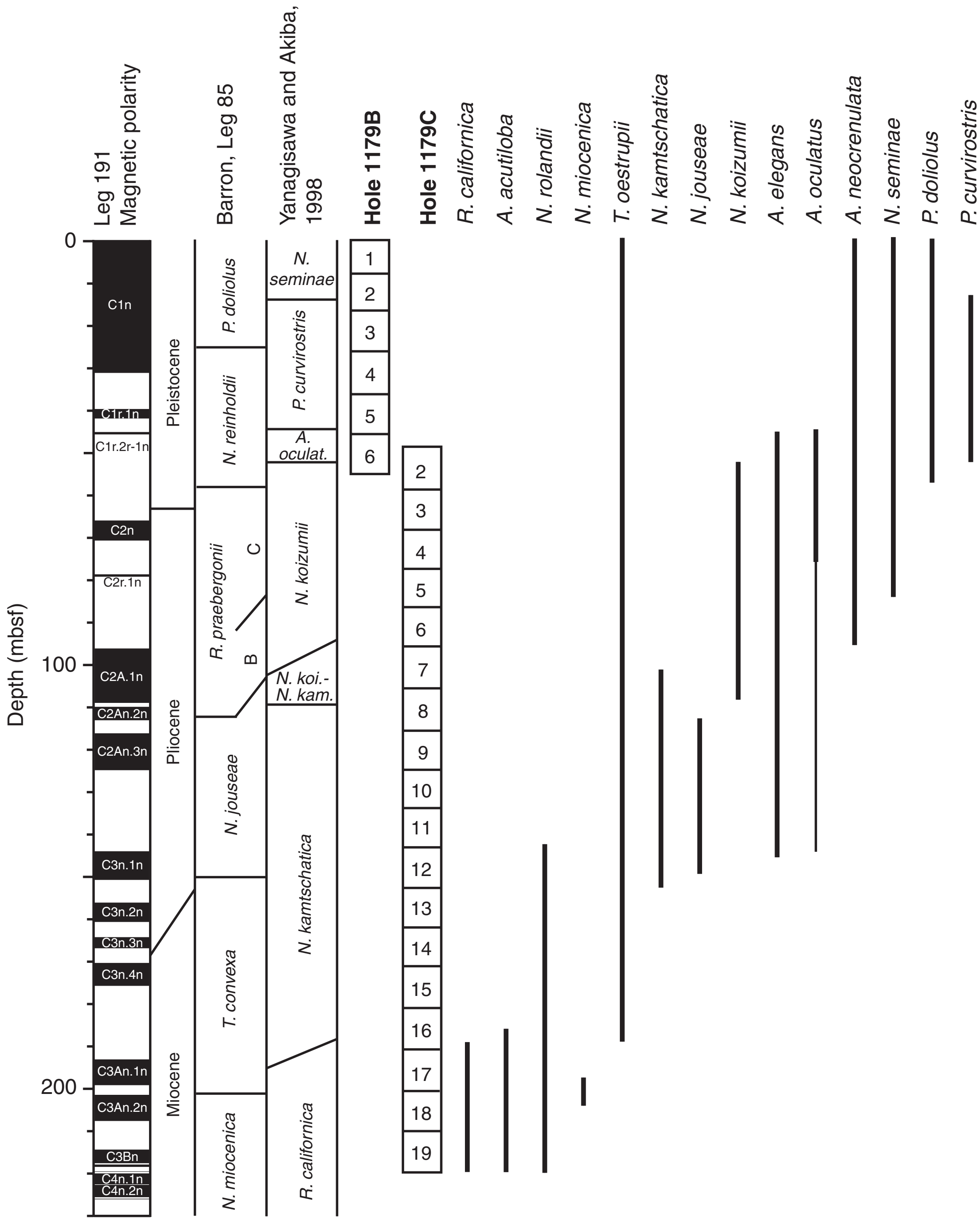

Figure F5. Site 1179 ash layer chronology developed from radiometric dating of ash layers and magnetic stratigraphy. Column at left shows Site 1179 cores; column in middle shows ash layers; column at right gives radiometric and magnetic ages (from Escutia et al., in press).

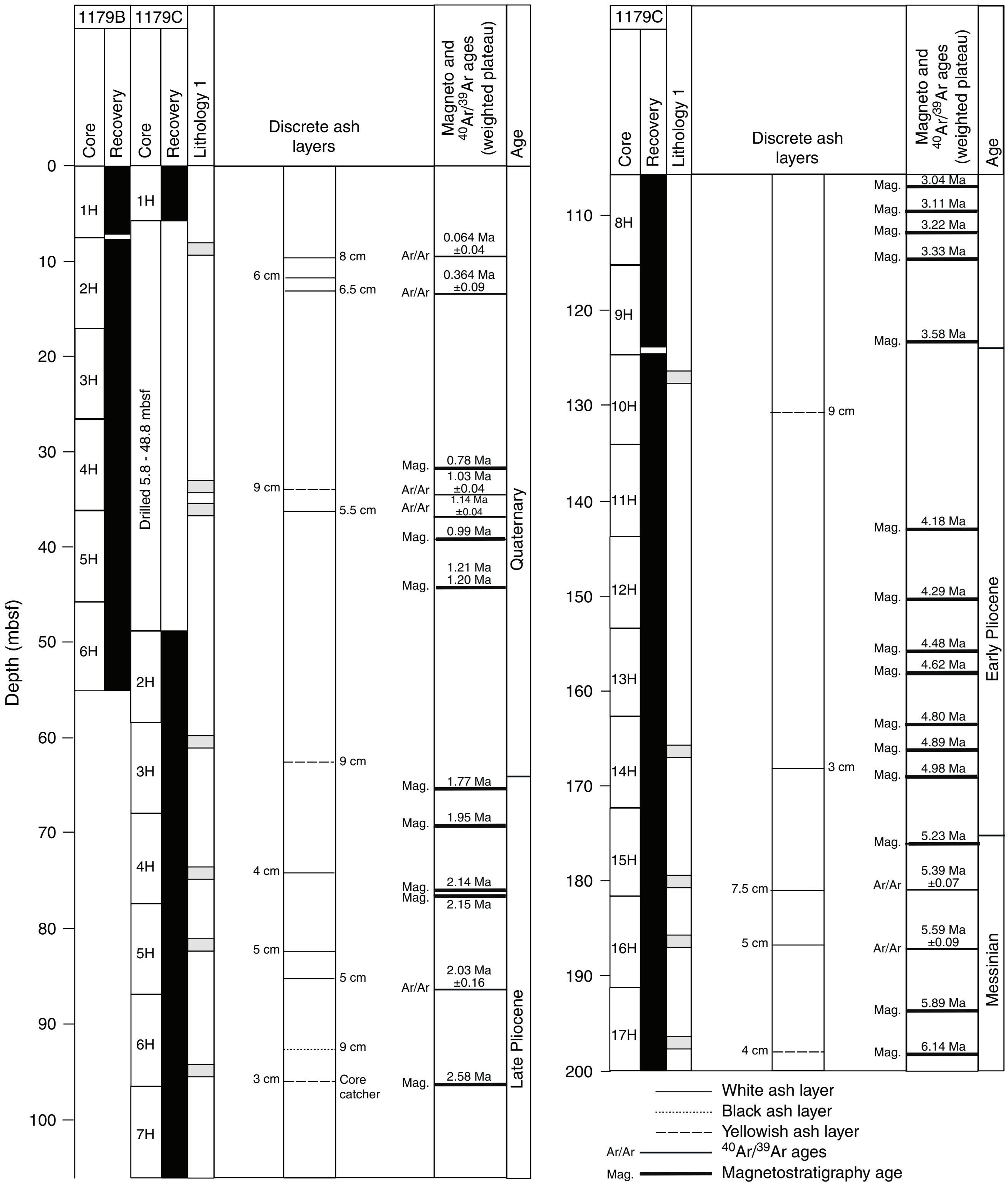

Figure F6. Cross plot of εNd(t) vs. $^{87}Sr/^{86}Sr$ for Site 1179 igneous samples (open and solid circles). Hachured areas show fields where samples from two oceanic plateaus and mid-ocean-ridge basalts (MORB) plot (from published studies) (from Sano and Hayasaka, this volume). EPR = East Pacific Rise.

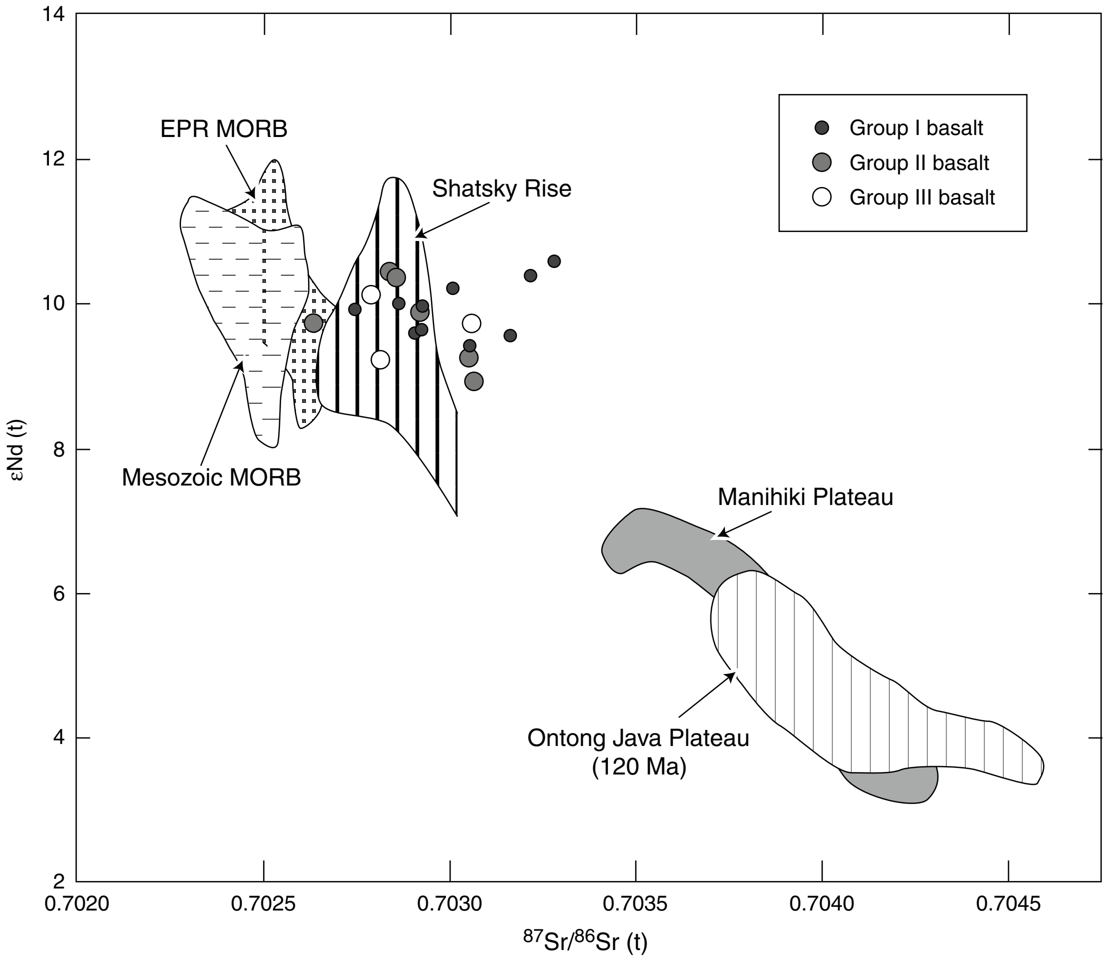

Figure F7. Measured colatitudes (from sample inclinations) and flow mean colatitudes plotted vs. depth in Hole 1179D. Open circles = individual sample colatitude values used to compute flow means; dots = sample colatitudes that were considered outlier values; solid squares = average colatitudes for 23 statistically distinct flow groups. Horizontal lines through these symbols = standard deviation of flow mean; italicized numbers with each mean colatitude symbol = the number of samples used to calculate that mean (in parenthesis); bold numbers give flow groupings considered to represent independent measurements of the geomagnetic field. Shaded areas show colatitudes that were considered serially correlated and therefore averaged in computing the 13 independent units. Dashed vertical line shows mean colatitude for site (from Sager and Horner-Johnson, this volume).